Int J Thermophys (2007) 28:958–967
DOI 10.1007/s10765-007-0227-6

Calorimetry of Nanophases of Macromolecules

Bernhard Wunderlich

Published online: 7 August 2007

Abstract The thermodynamic description of polymeric systems is summarized based on 50 years of gathering experimental information with adiabatic, differential-scanning, and temperature-modulated calorimetry. This experience has led to a description of macro- to micro- to nano-phases with macromolecules able to traverse the phase boundaries and decouple at the surfaces, resulting in different thermodynamic properties for the separated parts of the molecule. A typical thermodynamic characterization of semicystalline polymers is that of a globally metastable system with locally reversible processes. Unique phenomena in polymers include the ability of semicrystalline polymers to undergo cold crystallization and molecular nucleation, possess thermally generated point defects and rigid-amorphous fractions, and have amorphous to mesophasic to crystalline macroconformations with glass, ordering, and disordering transitions in all three structures. To describe such multifaceted systems, special combinations of equilibrium, and irreversible thermodynamics as well as statistical and quantum mechanics are necessary. Only then is it possible to handle violations of phase rules, changes of properties when approaching nanophase dimensions, local reversibility, and enthalpy relaxation. The enthalpy relaxation in polymers originates in the cooperativeness of conformational motion and the interferences of processes of different time scales. The experiments to identify the effects of

B. Wunderlich (✉)
Department of Chemistry, The University of Tennessee, Knoxville, TN 37996-1600, USA
e-mail: Wunderlich@CharterTN.net

B. Wunderlich
Chemical Sciences Division, Oak Ridge National Laboratory, Oak Ridge, TN 37831-6197, USA

the different molecular motions from typical vibrational time scales of picoseconds to cooperative, large-amplitude rearrangements of up to megaseconds span heating rates of thousands of $K \cdot s^{-1}$ with superfast chip calorimeters to many hours for slow, quasi-isothermal analysis by temperature-modulated differential scanning calorimetry (TMDSC). Selected examples of this far-reaching thermal characterization will be presented.

Keywords Calorimetry · Glass transition · Melting/crystallization · Microphase · Nanophase · Phase · Phase transition · Reversible decoupling · Superfast calorimetry

1 Introduction

More than 2,000 years ago the simple theory of matter from a human, macroscopic point of view consisted of four elements (fire, air, water, and earth) and two pairs of qualities (hot/cold and wet/dry). This scheme represents at the same time the basis of thermal analysis as expressed in today's logo of the International Confederation for Thermal Analysis and Calorimerty (ICTAC) [1]. Similarly, the linear and flexible macromolecules, commonly called polymers, are the most basic materials of life and of central importance for the understanding of nature as well as modern materials science [2]. While atoms and molecules were proven about 200 years ago to be the elemental particles of the macroscopically recognized matter [3] and their size and properties were well established during the last 100 years, the linear and flexible macromolecules were safely identified only 90 years ago [4]. Heat, the fourth "element" of antiquity was identified about 100 years ago as the energy of molecular motion [5]. This led to the development of "thermodynamics," a general theory for the description of all matter, energy, and the phase-structure [6].

Figure 1 summarizes the three size ranges of the thermodynamic phases. The macrophases represent the phases already described by Dalton in the form of his fluid (gaseous), liquid, and solid "bodies" [3]. Colloids, the first microphases, were discovered some 150 years ago [7], and the nanophases, the topic of this article, became "cutting-edge" research only some 20 years ago. This large spread of the milestones leading to the understanding of nanophases of polymers left many common expressions in science without a precise, operational definition [8]. In the field of polymer science, this led to many errors when one wanted to model these last recognized types of molecules on the earlier described small or large, but largely rigid molecules. The latter two types of molecules were the basic materials of the chemistry of the first half of the 20th century.

Figure 2 displays the types of phases recognized, including the mesophases with "intermediate" order in their structure [9]. In the development of the scheme of Fig. 2, structure *and* molecular motion were necessary to be considered for full description of both structure and properties. A solid, usually shows vibrational motion only, all other phases have added large-amplitude motion, where the large-amplitude motions consist of internal rotation, i.e., conformational motion, rotation, and translation.

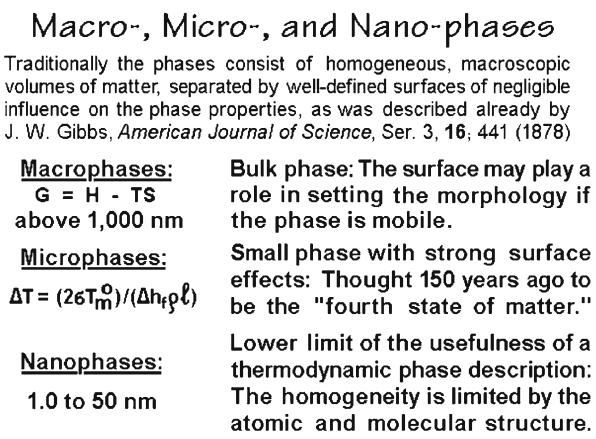

Fig. 1 Three size-ranges of the thermodynamic phases (G, H, and TS are the usual thermodynamic energy functions; ΔT, which expresses the lowering of the equilibrium melting temperature of a large crystal, $T_{\mathrm{m}}^{\mathrm{o}}$, is given by the Gibbs-Thomson equation, involving the specific surface free energy σ, the specific heat of fusion Δh_f, the density ρ, and the lamellar thickness ℓ).

2 Instrumentation

Quantitative measurements of heat began in the 18th century. Adiabatic calorimetry with today's precision began with Nernst's calorimeter [10]. In adiabatic calorimetry, a sample is heated in an adiabatic enclosure and the resulting change in temperature, ΔT, is measured. The heat absorbed can then be equated to the heat capacity, C_p, multiplied with ΔT. At the same time, heating and cooling curves were quantified to ultimately measure heat by differential thermal analysis (DTA) [11] using Newton's law of heating. With later automatic recording and control of temperature and temperature differences, this DTA led to differential scanning calorimetry (DSC) [12], and ultimately to temperature-modulated DSC (TMDSC) [13]. Adiabatic calorimetry and DSC yield thermodynamic functions when equilibrium is assured; polymeric systems, however, are often not even close to equilibrium, so that TMDSC is needed to check on the reversibility of phase transitions. Figure 3 finally illustrates the latest development in electronic chip calorimetry which can follow nonequilibrium processes with rates approaching $10^6\,\mathrm{K{\cdot}s^{-1}}$ [14]. As seen from the sample masses analyzed in Fig. 3, the increasingly faster heating rated are possible by correspondingly decreased masses. This decrease in mass is necessary to keep the temperature gradient created during the external heating or cooling within acceptable error limits [2]. The schematic of the chip calorimeter illustrates the exceedingly small sample speck of about 10 μm diameter. Needles to say, all of the types of calorimetry depend on precise measurement and error correction.

3 Results and Discussion

Figure 4 illustrates the relationships between glass, melt, and crystal, commonly seen in semicrystalline macromolecules. At a given temperature, the lowest free enthalpy,

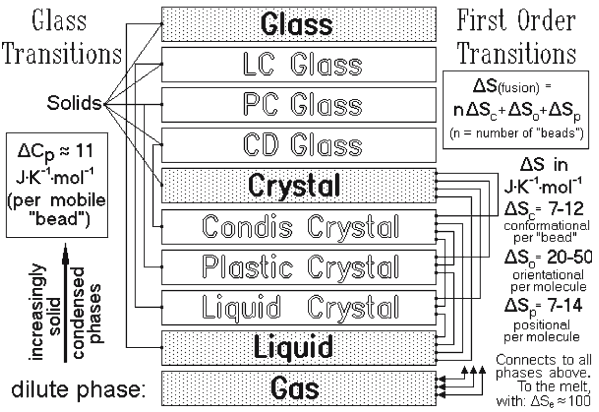

Fig. 2 Types of possible phases and their transitions based on molecular structure and mobility

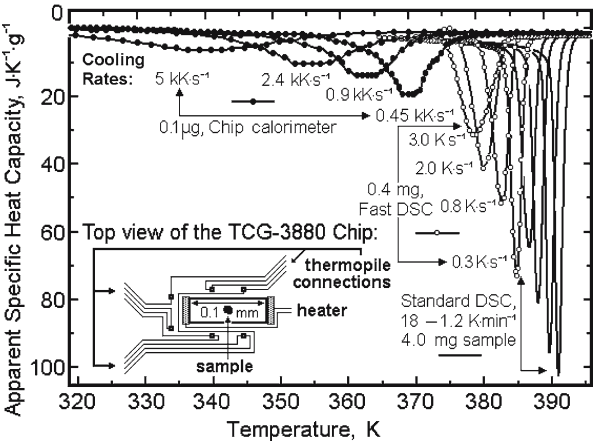

Fig. 3 Crystallization of polyethylene, PE, by cooling from the melt as determined by standard DSC, fast DSC, and electronic chip calorimetry which can follow nonequilibrium processes with rates to 10^6 K·min^{-1} [14]

G, represents equilibrium. From this free-enthalpy scheme and the summary of phases in Fig. 2, one can easily identify all glasses by the change in heat capacity at the glass transition temperature, T_g, which changes the curvature of G and, at the same time, marks the solidification of the liquid.[1] Crystals and the mesophases at the bottom of Fig. 2 have varying degrees of order and, thus, also different solidity. All mesophases have glass transitions [9], and it was shown that crystallization does not always increase

[1] Glass transitions are also called "brittle points" to mark a transition from the liquid to the solid state; furthermore, polymers reach a high viscosity of $\approx 10^{12}$ Pa·s at T_g.

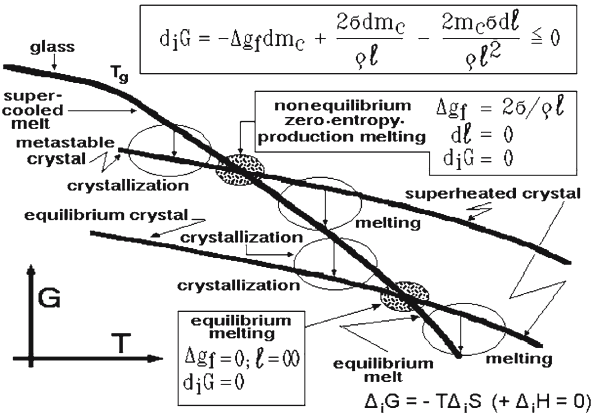

Fig. 4 Equilibrium and nonequilibrium for glassy, molten, and crystalline phases

T_g to coincide with T_m,[2] i.e., crystals may have a separate glass transition. In the monoclinic crystals of the poly(oxyethylene)s, T_g occurs almost 20 K *below* T_m [15].

Figure 5 displays details about the glass transition of amorphous and semicrystalline poly(ethylene terephthalate), PET [16]. The TMDSC is performed quasi-isothermally, i.e., by modulation about the indicated temperatures. A broadening of the transition on crystallization is clearly seen and indicates coupling of different parts of the same molecule across the phase boundary. Typical polymer molecules are of micrometer lengths and can easily bridge crystal phases through the amorphous phase. Of special interest is also the observation that the crystalline and amorphous fractions do not represent the complete sample. There is a third fraction which is noncrystalline, but does not participate in the glass transition. This rigid-amorphous fraction, RAF, was first quantitatively assessed by DSC for poly(oxymethylene) [17].

To continue the discussion of the phase transitions, one needs to recognize that in Fig. 4 all phases with free enthalpies vertically above those of the equilibrium melt or crystal are arrested equilibria and can only be analyzed using irreversible thermodynamics. First, one notes that there are two phase changes with zero-entropy production: at equilibrium, and where a metastable crystal changes to a melt with the same metastability. In the following equation for the melting of lamellar crystals (also listed in the figure):

$$d_i G = \Delta g_f dm_c + \frac{2\sigma\, \mathrm{d}m_c}{\ell} - \frac{2m_c \sigma\, \mathrm{d}\ell}{\rho \ell^2} \leq 0,$$

where $\mathrm{d}_i G$ is the free enthalpy production (linked in the closed system considered to the entropy production $\Delta_i S$, as shown in the bottom equation of the figure); Δg_f is the specific free-enthalpy change on fusion; σ is the specific surface free energy; ℓ is the

[2] In the case that the crystal is solid, melting absorbs not only the latent heat of fusion, characteristic of a first-order transition, but, in addition, the heat capacity changes from the value characteristic of a solid to that of a liquid, as in a glass transition.

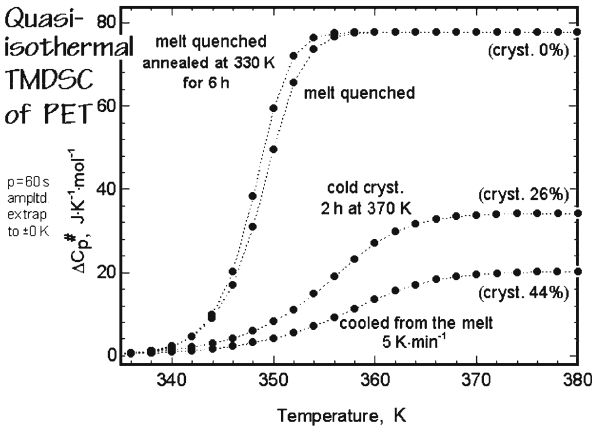

Fig. 5 Glass transitions of poly(ethylene terephthalates) (PET) of different thermal histories and crystallinities

lamellar thickness of the crystal; dm_c is the change in crystal mass; and ρ is the density [2]. The experimental determination of the zero-entropy production requires the wide range of heating rates illustrated in Fig. 3. Of the four downward arrows in Fig. 4 two indicate melting with superheating and two crystallization with supercooling, i.e., they mark permitted transitions with an entropy production.

The question of the dividing line between the micro- and nano-phases is resolved with the help of Fig. 6. Small spheres of polystyrene were analyzed by DSC [18]. The broadening of the glass transition by ≈50 K is interpreted as caused by increased mobility at the surface. By matching the heat capacities, the surface layer is about 5 nm thick, which in turn, suggests that a sphere with a radius of 5 nm would only be surface material and contains no bulk phase. The RAF in the semicrystalline polymers similarly must then be identified as a nanophase of properties different from the bulk-amorphous phase. These experiments support the summary of Fig. 1: macrophases have only negligible surface effects and are usually limited in size to dimensions larger than one micrometer. Microphases are affected in their properties by the surface, as indicated by the Gibbs-Thomson equation for the melting of thin, lamellar crystals which can be derived from the above equation by assuming no change in dℓ before melting and $\mathrm{d}_i G = 0$. Microphases still have a bulk phase in the center of their volume. The nanophases, finally, contain no bulk phase at all. The surface may cause a decrease in T_g (when the mobility increases at the interface) or an increase in T_g (when there is a stress transfer at the interface, as in the RAF). The upper limit of size of a nanophase, thus, is different for the different phase structures.

A comparison of standard calorimetry and TMDSC of the melting of polymers with extended-chain structure is shown in Fig. 7 for the example of a poly(oxyethylene). Quasi-isothermal TMDSC reveals that there is no reversible latent heat corresponding to the heat of fusion measured by standard DSC, even in the presence of crystal nuclei [19]. This is expected from the need of macromolecules to undergo molecular nucleation, proven earlier by the rejection of species shorter than the crystal-growing species at temperatures below their melting temperature [20].

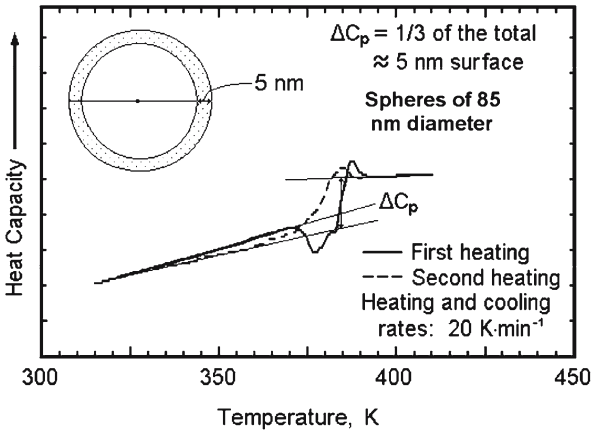

Fig. 6 Calculation of the surface volume of poly(styrene) to assess the lowering of the glass transition at the surface of small spheres based on DSC measurements. Note the ≈50 K shift of the beginning of the glass transition when going from the solid to the dashed line

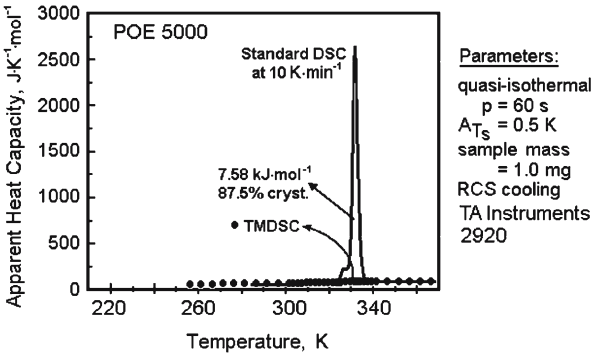

Fig. 7 Melting analysis by DSC and TMDSC which proves irreversible melting

Figure 8 illustrates the limit of reversible melting and crystallization of flexible paraffins and poly(ethylene)s. A distinct limit in length exists for the need to nucleate the molecule for crystallization [21]. The figure shows that this limit is much less than the beginning of large-scale chain folding which occurs when the number of backbone atoms, x, is about 250 [22].

The complete irreversibility of melting of polymers, suggested in Fig. 8, was shown to be limited to crystals of extended-chain and sharply-folded molecules. With quasi-isothermal TMDSC, it was discovered that a sizeable reversible melting exists in poly(ethylene terephthalate) [23]. By now, many other polymers are shown to have the same melting behavior [24]. These experiments point to a globally metastable structure for these semicrystalline polymers with some decoupled chain segments which melt locally in a reversible manner. The likely site of the reversible melting is at the growth front, established by the irreversible crystallization. The reversible melting is first seen at low temperature where it usually has high specific reversibility.

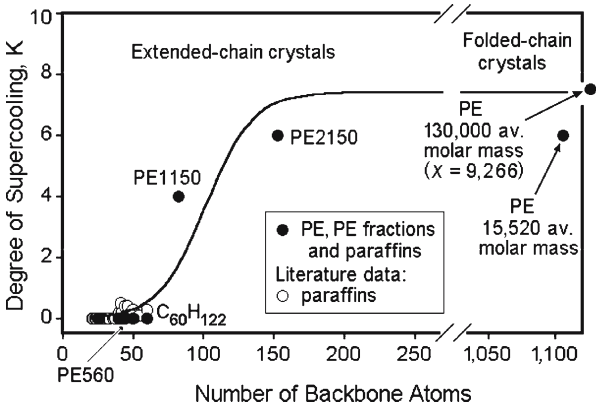

Fig. 8 Critical chain length for molecular nucleation for paraffins and polyethenes

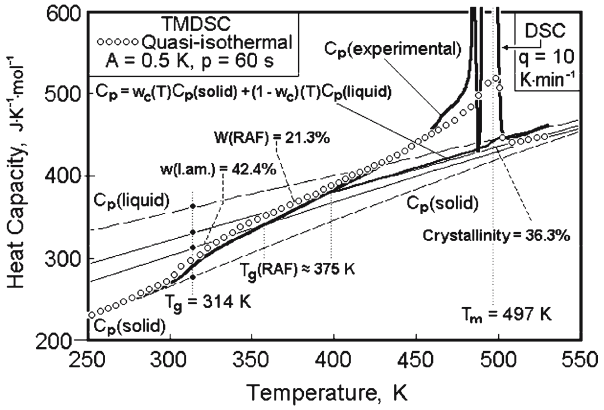

Fig. 9 Poly(butytlene terephthalate) analyzed by DSC and TMDSC

The specific reversibility drops to a much lower level when the irreversible melting-peak temperature is reached. The specific reversibility is the percentage of reversible melting, measured by quasi-isothermal TMDSC, relative to the total melting, measured by standard DSC, both over the same, narrow temperature range [25]. Total reversible melting, which is obtained by integration of the specific reversibility over the complete melting range, may reach 5–20% for homopolymers and 30–50% for copolymers. Less perfect crystallization with lower crystallinity usually leads to higher amounts of reversible melting.

Figure 9 summarizes a full analysis of the thermal behavior of a semicrystalline poly(butylene terephthalate) [26]. First, the heat capacities of the limiting states have to be determined as baselines for the quantitative analysis. Next, the two glass transitions must be evaluated to know the liquid amorphous, marked as (l.am.) in Fig. 9 and rigid amorphous fraction marked as (RAF) in Fig. 9. In the shown case the sample was cooled slowly for crystallization, so that the two glass transitions are well separated. Finally, the full DSC curves can be reproduced above T_g(RAF) using the following

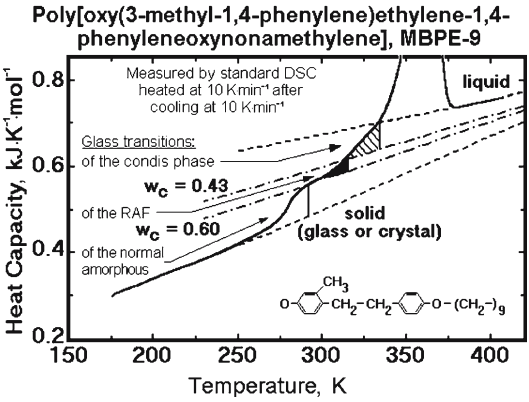

Fig. 10 Three glass transitions of MBPE-9

equation (also indicated in the figure):

$$C_{\mathrm{p}} = w_c(T) \quad C_{\mathrm{p}}(\mathrm{solid}) + (1 - w_c)(T) \quad C_{\mathrm{p}}(\mathrm{liquid}),$$

where C_p represents the overall heat capacity and w_c, the weight fraction of crystallinity. All quantities should be inserted with their proper temperature dependence. Quickly cooled samples can be analyzed analogosly with the known T_{g}(RAF). Superfast chip calorimetry can be used to check the limits of metastability [27].

Figure 10, finally, illustrates the changes which were found for the indicated multiblock copolymer MBPE-9, consisting of a rigid and a flexible segment [28,29]. In this case three glass transitions can be observed, one for the condis mesophase (see Fig. 2), one for the bulk-amorphous phase, and the intermediate one for the RAF.

4 Conclusions

On cooling from the melt, macromolecules are usually arrested in metastable states. Frequently even homopolymers separate into multi-phase structures which may have nanometer dimensions. In order to present a consistent picture of the calorimetric properties, it is necessary to extend the common description based on equilibrium thermodynamics to nonequilibrium states and their transition. A list of all types of phases in Fig. 2 is based on both structure *and* molecular motion, and permits easy separation into one dilute, mobile phase (the gas), four condensed solid phases (the glasses), and a group of five condensed phases of different mobility. It is important to recognize that in this description the glass transition and not the ordering is the key to the change of a mobile phase to a solid. Each phase may have three distinct sizes, as summarized in Fig. 1. With these basic descriptions, it is shown in Fig. 4 that the free-enthalpy diagram for a glass, melt, and crystal can be used to link the stability of equilibrium and nonequilibrium phases. Consisting of ordered and amorphous phases, both the glass transition, measured by determining the change in heat capacity, and the first-order transitions, judged by finding the entropy changes,

are accessible through thermal analysis with techniques which range from slow to superfast, as seen from Fig. 3. Figures 4–10, finally, illustrate some of the experiments clarifying the broadening of the glass transition due to stress transfer through the point of decoupling of molecules that traverse the crystal/amorphous interface, the evaluation of the RAF and its glass transition, the reversible and irreversible melting of crystals, and the possible multiple glass transitions.

Acknowledgment This work was supported by the Division of Materials Research, National Science Foundation, Polymers Program, Grant # DMR-0312233. Use of some equipment and laboratory space was provided by the Division of Materials Sciences and Engineering, Office of Basic Energy Sciences, U.S. Department of Energy at Oak Ridge National Laboratory, managed and operated by UT-Battelle, LLC, for the U.S. Department of Energy, under Contract Number DOE-AC05-00OR22725.

References

1. International Confederation for Thermal Analysis and Calorimetry (ICTAC); www.ictac.org/
2. B. Wunderlich, *Thermal Analysis of Polymeric Materials* (Springer, Berlin, 2005), and the parallel computer course of 3,000 screens of text, graphics, and hypertext (available by download from the ATHAS web site: http://athas.prz.rzeszow.pl, or www.scite.eu, and the European Virtual Institute for Thermal Metrology: www.evitherm.org/index.asp at their home page for thermal analysis and calorimetry)
3. J. Dalton, *A New System of Chemical Philosophy*, (London 1808); available as reprint from the: The Science Classics Library. Citadel Press, New York (1964)
4. H. Staudinger, Ber. dtsch. chem. Ges. **53**, 1073 (1920)
5. F. Bacon, *Novum Organum* speculated already: "...the very essence of heat, or the substantial self of heat is motion and nothing else" (1620)
6. H.A. Bumstead, R. Gibbs Van Name, The Scientific Papers of J. Willard Gibbs. Longmans, Green and Co., New York, 1906; reprinted (Dover Publications, New York, 1961)
7. T. Graham, Trans. Farad. Soc. (London) **151**, 183 (1861)
8. P.W. Bridgman, *The Logic of Modern Physics*. (MacMillan, New York, 1927)
9. B. Wunderlich, J. Grebowicz, Adv. Polym. Sci. **60/61**, 1 (1984)
10. W. Nernst, Sitzungsber. d. Preuss. Akad. Wiss. 247 (1910)
11. N.S. Kurnakov, Z. anorg. Chemie **42**, 184 (1904)
12. M.J. O'Neill, Anal. Chem. **36**, 1238 (1964)
13. P.S. Gill, S.R. Sauerbrunn, M. Reading, J. Thermal Anal. **40**, 931 (1993)
14. S.A. Adamovsky, A.A. Minakov, C. Schick, Thermochim. Acta **403**, 55 (2003)
15. W. Qiu, M. Pyda, E. Nowak-Pyda, A. Habenschuss, B. Wunderlich, Macromolecules **38**, 8454 (2005)
16. I. Okazaki, B. Wunderlich, J. Polym. Sci., Part B: Polym. Phys. **34**, 2941 (1996)
17. H. Suzuki, J. Grebowicz, B. Wunderlich, British Polym. J. **17**, 1 (1985)
18. U. Gaur, B. Wunderlich, Macromolecules **13**, 1618 (1980)
19. K. Ishikiriyama, B. Wunderlich, Macromolecules **30**, 4126 (1997)
20. B. Wunderlich, Disc. Farad. Soc. **68**, 239 (1979)
21. J. Pak, B. Wunderlich, Macromolecules **34**, 4492 (2001)
22. D.C. Bassett, R.H. Olley, S.J. Sutton, A.S. Vaughan, Macromolecules **29**, 1852 (1996)
23. I. Okazaki, B. Wunderlich, Macromolecules **30**, 1758 (1997)
24. B. Wunderlich, Progr. Polym. Sci. **28**, 383 (2003)
25. R. Androsch, B. Wunderlich, J. Polym. Sci., Part B: Polym. Phys. **41**, 2051 (2003)
26. M. Pyda, E. Nowak-Pyda, J. Mays, B. Wunderlich, J. Polym. Sci., Part B: Polym. Phys. **42**, 4401 (2004)
27. M. Pyda, E. Nowak-Pyda, J. Heeg, H. Huth, A.A. Minakov, M.L. Di Lorenzo, C. Schick, B. Wunderlich, J. Polym. Sci., Part B: Polym. Phys. **44**, 1364 (2006)
28. J. Cheng, Y. Jin, B. Wunderlich, S.Z.D. Cheng, M.A. Yandrasits, A. Zhang, V. Percec, Macromolecules **25**, 5991 (1992)
29. Y. Jin, J. Cheng, B. Wunderlich, S.Z.D. Cheng, M.A. Yandrasits, Polym. Advan. Technol. **5**, 785 (1994)